



This is a repository copy of *Identification of Coupled Map Lattice Models of Deterministic Parameter Models*.

White Rose Research Online URL for this paper:
<http://eprints.whiterose.ac.uk/83767/>

Monograph:

Billings, S.A. and Coca, D. (1999) Identification of Coupled Map Lattice Models of Deterministic Parameter Models. Research Report. ACSE Research Report 756 .
Department of Automatic Control and Systems Engineering

Reuse

Unless indicated otherwise, fulltext items are protected by copyright with all rights reserved. The copyright exception in section 29 of the Copyright, Designs and Patents Act 1988 allows the making of a single copy solely for the purpose of non-commercial research or private study within the limits of fair dealing. The publisher or other rights-holder may allow further reproduction and re-use of this version - refer to the White Rose Research Online record for this item. Where records identify the publisher as the copyright holder, users can verify any specific terms of use on the publisher's website.

Takedown

If you consider content in White Rose Research Online to be in breach of UK law, please notify us by emailing eprints@whiterose.ac.uk including the URL of the record and the reason for the withdrawal request.



eprints@whiterose.ac.uk
<https://eprints.whiterose.ac.uk/>

X

IDENTIFICATION OF COUPLED MAP LATTICE MODELS OF DETERMINISTIC DISTRIBUTED PARAMETER MODELS

S.A. BILLINGS



D. COCA

Department of Automatic Control and Systems Engineering,
University of Sheffield
Sheffield, S1 3JD,
UK

Research Report No. 756
September 1999



200452134



Identification of Coupled Map Lattice Models of Deterministic Distributed Parameter Systems

S.A. BILLINGS D. COCA

Department of Automatic Control and Systems Engineering,
University of Sheffield,
Sheffield S1 3JD, UK

Abstract

This paper introduces a novel approach to the identification of Coupled Map Lattice models of linear and nonlinear infinite-dimensional systems from discrete observations. The method exploits the regularity of the Coupled Map Lattice model so that only a finite number of spatial measurements are required. The measurement system associated with a CML is discussed and some necessary conditions for the input/output equations to form a CML are presented. Numerical simulations are used to illustrate the applicability of the proposed method.

1 Introduction

Modelling and characterisation of spatially extended systems, also known as *Distributed Parameter Systems* (DPS), is of great importance for understanding the dynamics of many physical, chemical and biological systems.

Unlike lumped parameter dynamical systems, which can be described in terms of a finite set of Ordinary Differential Equations (ODEs), DPS are infinite dimensional in most common realisations. For example, the evolution of spatially extended systems is very often described in terms of linear or nonlinear Partial Differential Equations (PDE's).

The analysis, simulation and control of infinite dimensional systems described by partial differential equations presents many computational and theoretical difficulties. Stability analysis and optimal control of PDEs [2] is still a very difficult problem in mathematics. In addition, the computation and implementation of the control laws is complicated by the infinite dimensionality of the state space.

For these reasons, in most practical situations the original infinite dimensional system modelled in terms of PDEs is approximated by a finite dimensional dynamical system, described by ODEs or difference equations. The accuracy of the original model is sacrificed in this case for the sake of simplicity of the finite dimensional model.

A finite-dimensional model of the distributed parameter system can be obtained by approximating the infinite dimensional state-space using finite-dimensional eigensubspaces [13]. Often however the eigensubspaces are not known a priori and are difficult if not impossible to compute.

An alternative approach that does not require spectral decomposition is the finite-element method (FEM) [7] based on the Galerkin method for solving PDEs. This method involves approximating the space where the solution of the PDE is sought in terms of elementary basis

functions.

The partial differential operator can also be approximated using finite differences. Using the finite difference method a PDE can be mapped onto a Coupled Lattice Map (CML) model, which is discrete in time and space and, unlike Cellular Automata models, has a continuous state [24].

Due to their computational efficiency and richness of dynamical behaviour, the CML models have in recent years become a very active research area. Research into CML models was initiated in the 80's by K Kaneko [21], [22]. Using computer simulations, Kaneko revealed that coupled map lattices can exhibit surprisingly rich dynamical behaviour, including spatio-temporal chaos and intermittency, traveling waves and pattern formation [23]. Because of their computational efficiency and ability to reproduce complex spatio-temporal behaviour, CML models have emerged as an effective and powerful tool to study nonlinear distributed parameter systems. In particular, CML have been used to model convected temperature fluctuations in the atmosphere [31], boiling processes [35] and spatio-temporal chaos in fluid flows [17].

The applicability of CML in modelling distributed parameter systems is actually much broader, as such models are particularly suited to model spatially discrete phenomena involving the interaction and propagation of large ensembles of elementary oscillations which normally cannot be modelled using PDEs [12]. Examples of such phenomena include pulse propagation in excitable arrays of cells composing myelinated nerve fibers or myocardial tissue [1] [26], chemical reactors coupled by mass exchange [6], neuronal activity in the visual cortex [16], coupled Josephson junction [10] and laser arrays [30].

Despite the considerable attention devoted to Coupled Map Lattices, a crucial problem that has not been addressed so far is the identification of CML models of spatially extended systems directly from data. Given the importance and wide applicability of such models both for theoretical studies and practical applications, obtaining the finite-dimensional Coupled Map Lattice model of an unknown distributed parameter system can be an essential part in any attempt to understand, analyse or control the distributed system.

The aim of this paper is to introduce a methodology to identify the CML equations that approximate the dynamics of a linear or nonlinear infinite dynamical system using only a finite set of observations recorded from sensors distributed in the spatial domain. The novel approach presented here is related to nonlinear system identification methods for deterministic and stochastic nonlinear dynamical systems, based on NARX and NARMAX models [28], [27].

The proposed method exploits the particular characteristics of the Couple Map Lattice architecture to reduce the complexity of the identification task, which otherwise, given the infinite-dimensionality of the dynamical systems involved, would be computationally prohibitive.

The paper is organised as follows. Section 2.1 introduces some general concepts regarding Lattice Dynamical Systems (LDS). Restrictions to the general LDS model are discussed in Section 2.2 and Section 2.3 where a rigorous definition of the CML is given.

Section 3.1 contains a brief review of the NARMAX method. In Section 3.2 some conditions for the measurement system associated with a CML, which guarantee that the resulting input/output equations define a CML, are discussed. The new identification methodology for deterministic CML models is introduced in Section 3.3. Simulation results which illustrate the applicability of the proposed approach are presented in Section 4.

2 Theory and Definitions

Coupled Map Lattices are a special class of spatially distributed, interacting dynamical systems known as Lattice Dynamical Systems (LDS).

2.1 Lattice Dynamical Systems

A Lattice Dynamical System is a spatially extended dynamical system composed of a finite or infinite number of interacting dynamical systems, each assigned to a node of a one- or multi-dimensional lattice of integers representing a discretisation of the physical space.

The dynamics of a LDS can be viewed as a combination of local dynamics, involving the local state-space variables assigned to every lattice node, and spatial interactions, which usually involve dynamical state-space variables associated to neighbouring lattice nodes although non-local or even global coupling is also permitted.

A fundamental characteristic of LDSs is the fact that the local state-space variables associated to each lattice node or spatial location are the same over the given lattice, that is, represent the same set of physical quantities such as pressure, temperature, velocity etc. This feature distinguishes a Lattice Dynamical System from a more general n -dimensional dynamical system.

Depending on whether the time variable t is continuous or discrete, Lattice Dynamical Systems can be classified into two categories, continuous-time Lattice Dynamical Systems represented as finite or infinite dimensional systems of ordinary differential equations

$$\frac{dx_i}{dt} = f_i(x, u), \quad t \in \mathbb{R}_+, i \in \mathbb{Z}^d, d \geq 1 \quad (1)$$

and discrete-time Lattice Dynamical Systems described in terms of difference equations

$$x_i(t) = f_i(q^{n_x} x(t), q^{n_u} u(t)), \quad t \in \mathbb{Z}_+, i \in \mathbb{Z}^d, d \geq 1 \quad (2)$$

In the above equations $f_i : \mathcal{X} \times \mathcal{U} \rightarrow \mathcal{X}$ is a differentiable map, $x_i(t) \in \mathcal{X}_i \subset \mathbb{R}^l$ and $u_i(t) \in \mathcal{U}_i \subset \mathbb{R}^l$ are l -dimensional vectors representing the local state-space and input variables respectively at the i th node of the lattice $\mathcal{I} \subset \mathbb{Z}^d$, $x \in \mathcal{X}$ and $u \in \mathcal{U}$ are the global, finite or infinite dimensional, state-space variable and input vectors. In general, the lattice \mathcal{I} is the set of all integer coordinate vectors $i = \{i_1, \dots, i_d\} \in \mathbb{Z}^d$.

In equation (2) q^n is a multi-valued backward shift operator

$$q^n = (q(-1)q(-2)\dots q(-n)) \quad (3)$$

where

$$q(-j)x(t) = x(t-j) \quad (4)$$

and n_x and n_u are the maximum time-lags corresponding to x and u .

2.2 Simplifications of the general LDS model

The general LDS model can be simplified considerably by introducing a certain degree of regularity and symmetry into the equations describing the LDS.

In the general model (1) each site can be coupled with all the other sites in the lattice, this represents a globally coupled LDS. Very often however the spatial interactions are restricted to only a finite set of lattice nodes such that equations (1) and (2) can be rewritten as

$$\frac{dx_i}{dt} = f_i(x_i, u_i, s_i^m x_i, s_i^m u_i), \quad t \in \mathbb{R}_+, \quad i \in \mathbb{Z}^d, \quad d \geq 1 \quad (5)$$

for the continuous-time LDS model and

$$x_i(t) = f_i(q^{n_x} x_i(t), q^{n_u} u_i(t), s_i^m q^{n_x} x_i(t), s_i^m q^{n_u} u_i(t)), \quad t \in \mathbb{Z}_+, \quad i \in \mathbb{Z}^d, \quad d \geq 1 \quad (6)$$

the discrete-time LDS model respectively,

In the above equations

$$q^{n_x} x_i(t) = (x_i(t-1) \dots x_i(t-n_x)) \quad (7)$$

$$q^{n_u} u_i(t) = (u_i(t-1) \dots u_i(t-n_u)) \quad (8)$$

and s_i^m is a multi-valued spatial shift (translation) operator

$$s_i^m = (s(p_1^i) s(p_2^i) \dots s(p_m^i)) \quad (9)$$

such that

$$s_i^m x_i = (x_{i-p_1^i} \dots x_{i-p_m^i}) \quad (10)$$

where $p^i = \{p_j^i\}$, $p_j^i \in \mathbb{Z}^d$, is a spatial translation multi-index.

The extent of the spatial interactions in the LDS model can be quantified in terms of the size or radius r_i of the coupling neighbourhood, which indicates the most distant spatial interaction for each lattice site

$$r_i = (r_i(1), \dots, r_i(d)) = (\max_{j=1, \dots, m} p_j^i(1), \dots, \max_{j=1, \dots, m} p_j^i(d)) \quad (11)$$

As a simplification of the general LDS model, the lattice equations can be assumed spatially invariant over the entire lattice. This means that the differential or difference equations corresponding to each lattice node are the same for all lattice nodes such that $f_i = f$, $s_i^m = s^m$, $r_i = r$ for $i \in \mathcal{I}$.

Often, the the map f can be decomposed into a *local map* f_l involving only the local state-space variable x_i and a *coupling map* f_c which describes the interactions with neighbouring lattice sites

$$f(x_i, u_i, x_{i-p_1}, \dots, x_{i-p_m}, u_{i-p_1}, \dots, u_{i-p_m}) = f_l(x_i, u_i) + f_c(s^m x_i, s^m u_i) \quad (12)$$

When f is polynomial, for example, it is always possible to decompose f as follows

$$f(x_i, u_i, x_{i-p_1}, \dots, x_{i-p_m}, u_{i-p_1}, \dots, u_{i-p_m}) = f_l(x_i, u_i) + f_c(x_i, u_i, s^m x_i, s^m u_i) \quad (13)$$

where the polynomial f_l involves only the variables x_i and u_i while the polynomial f_c involves the coupling variables $s^m x_i$ and $s^m u_i$ and also, in a cross-product combination with the coupling variables only, the variables x_i and u_i .

Depending on the spatio-temporal system that is modelled, additional symmetry can be imposed on the coupling topology and the coupling function.

For a symmetric coupling topology $m = 2m'$ and

$$p_j = -p_{m-j+1}, \quad j = 1, \dots, m' \quad (14)$$

In addition, the coupling function f_c in (13) can be symmetric with respect to the coupling variables such that

$$f_c(x_i, u_i, x_{i-p_1}, \dots, x_{i-p_m}, u_{i-p_1}, \dots, u_{i-p_m}) = f_c(x_i, u_i, x_{i-p_m}, \dots, x_{i-p_1}, u_{i-p_m}, \dots, u_{i-p_1}) \quad (15)$$

or anti-symmetric when

$$f_c(x_i, u_i, x_{i-p_1}, \dots, x_{i-p_m}, u_{i-p_1}, \dots, u_{i-p_m}) = -f_c(x_i, u_i, x_{i-p_m}, \dots, x_{i-p_1}, u_{i-p_m}, \dots, u_{i-p_1}) \quad (16)$$

Diffusion processes for example, are generally modelled using symmetric coupling functions while anti-symmetric coupling is associated with the modelling of open flows.

In many practical situations the dynamics develops on a bounded spatial domain $\Omega \subset \mathbb{R}^d$ which leads to a finite-dimensional LDS, that is, $\mathcal{I} \subset \mathbb{Z}^d$ is a finite dimensional lattice.

For spatially bounded LDS dynamics, equations (5) and (6) are complemented with boundary conditions

$$B_\Gamma(x_i) = 0, \quad i \in \mathcal{I}_\Gamma \quad (17)$$

where \mathcal{I}_Γ contain all lattice points on the boundary of the spatial domain. Examples of boundary conditions are Dirichlet, Neumann or periodic boundary conditions.

2.3 The CML model

The following definition of a CML is assumed throughout the rest of this paper.

A Coupled Map Lattice is a discrete-time, spatially invariant LDS, with $f_i = f$ for all $i \in \mathcal{I}$, symmetric coupling topology of finite radius and symmetric or anti-symmetric coupling functions.

The CML model can be written as

$$x_i(t) = f_l(q^{n_x} x_i(t), q^{n_u} u_i(t)) + f_c(q^{n_x} x_i(t), q^{n_u} u_i(t), s^m q^{n_x} x_i(t), s^m q^{n_u} u_i(t)) \quad (18)$$

where the coupling topology s^m is symmetric (14) and the coupling function f_c is symmetric (15) or anti-symmetric (16).

One of the best known CML model consists of a chain of, diffusively coupled, chaotic logistic maps

$$x_i(t) = (1 - \epsilon)f(x_i(t-1)) + \epsilon/2[f(x_{i-1}(t-1)) + f(x_{i+1}(t-1))] \quad (19)$$

where f is the logistic map

$$f(x) = 1 - \lambda x^2 \quad (20)$$

This model was shown to generate a large variety of spatio-temporal phenomena [22]. The observed dynamical behaviour found in this system, most of which was originally unknown, is surprisingly complex, ranging from frozen random patterns and pattern competition to intermittency and fully developed spatio-temporal chaos [23].

CML can be used to model dynamical behaviour that normally is described by partial differential equations or by chains of coupled differential equations. CML models however, can exhibit a richer spectrum of dynamical behaviour than can be found in PDEs. The study of Coupled Lattice Maps led to the introduction of qualitatively new classes of dynamical behaviour for spatially extended systems. Some of the predicted dynamics were later identified in experimental systems.

Typical phenomena that does not occur in a spatially continuous model include wave propagation failure, [25] a phenomenon that can be associated for example with the failure of a traveling pulse to propagate along a nerve fiber or in cardiac tissue. Such systems can naturally be modelled as spatially discrete arrays of interacting cells [26].

From this point of view, CML's models are equally efficient in modelling systems that traditionally have been described in terms of Partial Differential Equations (PDE's), systems that are inherently discrete in space such as chains of coupled oscillators or arrays of Josephson junctions and systems that are discrete both in space and time such as ecosystem dynamics [32].

Obviously the CML model has limitations to modelling certain classes of spatio-temporal behaviours. The restrictions are mainly due to the regularity of the CML model. In practice the invariance across the lattice of the coupling function and coupling topology does not account for the nonuniformities occurring in some real-life systems. In the context of the nerve impulse transmission process for example, such nonuniformities could correspond to changes in the diameter of a nerve axon or in the conduction properties of the propagating medium. The physical phenomena induced by such nonuniformities include propagation delay and wave reflection [20], [36]. These systems can be modelled using the more general LDS (1).

3 System Identification of CML Models

Given the effectiveness of Coupled Map Lattices in modelling complex spatio-temporal dynamics it is clearly important to develop procedures which can recover the mathematical equations of CML models from patterns of data.

In the past decade the NARMAX method has been established as a powerful approach to the identification of nonlinear, lumped parameter, dynamical systems.

Recently [11], an extension of this method was developed to accommodate the identification of distributed parameter systems. The new approach was based on a finite-element approximation of the spatial domain in order to reduce the infinite dimensional identification problem to the identification of an approximate finite-dimensional dynamical system that can accurately reproduce the extended dynamical behaviour.

The method was designed to deal with infinite dynamical systems evolving over a continuous spatial domain, normally described in terms of PDEs. As noted above, many spatio-temporal systems are spatially-discrete, such as chains of coupled oscillators. These systems can easily be described using the CML formalism but not by PDEs so, from this point of view, the identification of CML models applies to a wider class of spatio-temporal dynamics.

The new identification approach is an adaptation of the NARXMAX (NARX for deterministic systems) method for the CML identification task. The principles of the original method remain but the identification methodology has to be modified to accommodate the particularities of the CML architecture.

3.1 The NARMAX Method Revised

Consider a discrete-time dynamical system described by the difference equations

$$x(t+1) = g(x(t), u(t)) \quad (21)$$

$$y(t) = h(x(t), u(t)) \quad (22)$$

in which the state x belongs to a n -dimensional vector space \mathcal{X} , the input u belongs to an m -dimensional vector space \mathcal{U} and the output y belongs to an l -dimensional vector space \mathcal{Y} . The vector field $g : \mathcal{X} \times \mathcal{U} \rightarrow \mathcal{X}$ and the output map $h : \mathcal{X} \times \mathcal{U} \rightarrow \mathcal{Y}$ are assumed to be real valued smooth functions.

Frequently, dynamical systems are characterised in terms of the *input/output behaviour* which illustrates the effects the inputs $u \in \mathcal{U}$ have on the system's outputs $y \in \mathcal{Y}$. Useful representations for the input/output behaviour of a dynamical system include the *Fliess functional expansion* and the *Volterra series expansion* in which the output y of the nonlinear system (21) is expressed as a functional of the input u in the form of a infinite series expansion.

Very often the only information available from an unknown dynamical system are input and output measurements, $u^N = [u(1), u(2), \dots, u(N)]$ and $y^N = [y(1), y(2), \dots, y(N)]$ respectively. The identification problem involves finding a parsimonious model of the system, which can reproduce accurately the observed input/output behaviour. This is closely related to the realisation problem in the theory of dynamical systems [19], [34].

The search for a discrete-time dynamical system which realises a given input/output behaviour involves determining the input/output equation, known as the NARX model [28],

$$y(t) = f(y(t-1), \dots, y(t-n_y), u(t-1), \dots, u(t-n_u)) \quad (23)$$

which, under some mild conditions, can be associated to the state-space representation (21). The stochastic equivalent of (23) defines the NARMAX model [27], which includes measurement noise $e(t)$ as part of the model

$$y(t) = f(y(t-1), \dots, y(t-n_y), u(t-1), \dots, u(t-n_u), e(t-1), \dots, e(t-n_e)) + e(t) \quad (24)$$

As before, \mathcal{Y} and \mathcal{U} are l - and m -dimensional vector spaces respectively. The main difference is that the output y in (24) is now a vector of random variables.

In the above equations $f : \mathcal{Y}^{n_y} \times \mathcal{U}^{n_u}$ is an unknown nonlinear mapping, n_y and n_u represent the maximum output and input lags, $e(t)$ is an unknown stochastic variable, assumed to be bounded $|e(t)| < \delta$ and uncorrelated with the input, and n_e the maximum lag of $e(t)$. The random variable $e(t)$ is the prediction error or innovation at time t for the stochastic system (24).

The most difficult problem in nonlinear system identification is determining the structure or architecture of the model. Assuming that no a priori knowledge of the form of the nonlinear functional f is available, a practical solution is to approximate f from the available data using a known set of basis functions or regressors

$$\mathcal{M} = \{g_k\}_{k=1}^M \subset \mathcal{F} \quad (25)$$

belonging to a given function class \mathcal{F} . Typical regressor classes used in nonlinear system identification include polynomial and rational functions, radial basis functions (RBF) and wavelets.

Typically, equation (23) is approximated as a linear expansion in terms of the basis functions (25)

$$y(t) = \sum_{k \in K} \theta_k g_k(y(t-1), \dots, y(t-n_y), u(t-1), \dots, u(t-n_u)) \quad (26)$$

selected from the considerably larger regressors set \mathcal{M} . In equations (25) and (26) K is the index of selected regressors.

The structure determination for NARX and NARMAX models (23) (24) is based on the Orthogonal Forward Regression (OFR) algorithm. This least-squares type algorithm is used to select the relevant regressors in equation (26), according to their importance as measured by the Error Reduction Ratio (ERR) criterion [4]. The algorithm also produces the least-squares estimate of the corresponding parameter vector $\Theta = \{\theta_k\}$ in (26).

3.2 CML input/output models

It is natural to consider a measurement system for the spatio-temporal system described by the CML model (18). Practically, this concerns the number, spatial distribution of the measurement sensors and the form of measurement equation associated to the state-space CML model (18)

$$y_i(t) = h_i(x, u) \quad (27)$$

with $h_i : \mathcal{X} \times \mathcal{U} \rightarrow \mathcal{Y}_i$ and $i \in \mathcal{I}$.

The input/output equation corresponding to the state-space CML model (18) with the output equation (27), if this exists, is not necessarily a CML model as defined in Section 2.3. Assuming that the dimension of the output vector equals the size of the CML lattice, the resulting input/output equations will form a general LDS. In this case, identifying the resulting LDS model requires the full input and output vectors.

In practice however, a number of mild additional assumptions regarding the measurement process can be made to ensure that the input/output equations corresponding to (18) and (27) form a CML. A consequence of this is that the resulting CML model can be identified using a very small number of inputs and outputs.

A reasonable assumption is that the same measurement devices are used at each spatial location so that $h_i = h$ are identical at each lattice node. It is also natural to expect that the measurement function will depend only on a finite number state and input variables in the neighbourhood of the measurement location that is

$$y_i(t) = h(x_i(t), u_i(t), s^k x_i(t), s^k u_i(t)) \quad (28)$$

But this still does not guarantee that the resulting input/output equation is a CML. A number of sufficient conditions are proposed below.

Proposition 1: *Given the CML equations (18) with symmetric coupling function and the measurement equation (28) the corresponding input/output equations define a CML if*

$$h(x, u) = h(x_i) \quad (29)$$

with h one-to-one on \mathcal{X}_i .

Proof

Subject to (29), the equivalent input/output equation of (18) given (28), at the i th node, is

$$y_i(t) = h(f_i(q^{n_x} h^{-1}(y_i(t)), q^{n_u} u_i(t)) + f_c(q^{n_x} h^{-1}(y_i(t)), q^{n_u} u_i(t), s^m q^{n_x} h^{-1}(y_i(t)), s^m q^{n_u} u_i(t))) \quad (30)$$

In equation (30) $h^{-1} : \mathcal{Y}_i \rightarrow \mathcal{X}_i$ is the inverse of the measurement function (29).

It is obvious that in (30) the symmetry of the coupling topology is preserved. Moreover, if f_c is symmetric (15)

$$h(f_i(q^{n_x} h^{-1}(y_i(t)) q^{n_u} u_i(t)) + \quad (31)$$

$$f_c((q^{n_x} h^{-1}(y_i(t)), q^{n_u} u_i(t), q^{n_x} h^{-1}(y_{i-p_1}(t)), \dots, q^{n_x} h^{-1}(y_{i-p_m}(t)), \quad (32)$$

$$q^{n_u} u_{i-p_1}(t), \dots, q^{n_u} u_{i-p_m}(t))) = \quad (33)$$

$$h(f_i(q^{n_x} h^{-1}(y_i(t)) q^{n_u} u_i(t)) + \quad (34)$$

$$f_c((q^{n_x} h^{-1}(y_i(t)), q^{n_u} u_i(t), q^{n_x} h^{-1}(y_{i-p_m}(t)), \dots, q^{n_x} h^{-1}(y_{i-p_1}(t)), \quad (35)$$

$$q^{n_u} u_{i-p_m}(t), \dots, q^{n_u} u_{i-p_1}(t))) \quad (36)$$

which means that h is symmetric and therefore the discrete-time Lattice Dynamical System defined by (30) is a CML.

Proposition 2: *Given the CML equations (18), with $f_i \equiv 0$ and anti-symmetric coupling function, and the measurement equation (28) the corresponding input/output equations define a CML if*

$$h(x, u) = h(x_i) \quad (37)$$

with h one-to-one on \mathcal{X}_i and

- h is an odd or even function that is

$$h(-x) = h(x) \text{ or } h(-x) = -h(x) \quad (38)$$

Proof

In this case, subject to (37), the resulting input/output equation at the i th node

$$y_i(t) = h\left(f_c\left(\mathbf{q}^{n_x} h^{-1}(y_i(t)), \mathbf{q}^{n_u} u_i(t), \mathbf{s}^m \mathbf{q}^{n_x} h^{-1}(y_{i-p_1}(t)), \mathbf{s}^m \mathbf{q}^{n_u} u_i(t)\right)\right) \quad (39)$$

clearly preserves the symmetry of the coupling topology \mathbf{s}^m . In addition, given f_c anti-symmetric and from (38) it follows that h is either a symmetric or anti-symmetric coupling function. Hence equation (39) defines a CML.

The input/output equations (30) or (39), for $i \in \mathcal{I}$ define a special type of multi-variable NARX model that has a regular lattice structure. A new class of nonlinear system identification techniques, that exploit the special properties of these type of models, is developed and tested in the following sections.

3.3 System Identification of Deterministic CML's

CML models have been used successfully to simulate distributed parameter systems described in terms partial differential equations. The common approach has been to convert the known PDE into a CML model using finite-difference approximation methods.

A different approach to obtain the CML model from data using system identification techniques is proposed here. The noise-free data required for identification can be generated by numerically integrating the PDE using an accurate numerical method such as the finite-element method for example. System identification, can then be used to determine the CML realisation of the simulated input/output behaviour. The resulting model is usually more accurate and stable than the similar model obtained using a straightforward finite-difference approximation.

This is one reason why it is important to investigate the identification of the CML models in the deterministic (noise-free) as well as in the stochastic context. It can also be argued that there are other practical situations when the data can be measured with very high accuracy or when data pre-processing has successfully eliminated measurement noise.

Consider the CML model (18) augmented with the measurement equations (28) such that the resulting input/output equations form a CML.

Identifying the input/output equations from data following the system identification methodology of MIMO-NARX models [4] requires the global input and output vectors $u = \{u_i\}$ and $y = \{y_i\}$ to be available for measurement. In practice the lattice size can be very large, possibly involving hundreds of equations. This makes the standard identification procedure computationally prohibitive. Moreover, often it is very expensive or impossible to measure the input/output vectors at every lattice site.

To overcome these difficulties, an alternative approach to the identification of CML models, which involves only a small number of measurement locations, is investigated here.

Consider the following nodal CML input/output equation

$$y_i(t) = F(\mathbf{q}^{n_y} y_i(t), \mathbf{q}^{n_u} u_i(t), \mathbf{s}^m \mathbf{q}^{n_x} y_i(t), \mathbf{s}^m \mathbf{q}^{n_u} u_i(t)) \quad (40)$$

where F is an unknown nonlinear mapping.

Because of the regularity of the lattice model, the identification of the CML input/output equation can be reduced to the identification of equation (40) given the input and output measurements at the i th lattice site $u_i^N = (u_i(1) \dots u_i(N))$ and $y_i^N = (y_i(1) \dots y_i(N))$ and from neighbouring lattice nodes $s^m u_i^N = (s^m u_i(1) \dots s^m u_i(N))$ and $s^m y_i^N = (s^m y_i(1) \dots s^m y_i(N))$. For the identification purpose the output measurements $s^m y_i^N$ can also be viewed as inputs in equation (40).

The number of measurement locations and therefore the number of sensors required is much smaller in this case, depending only upon the size of the coupling neighbourhood.

Usually no a priori information is available regarding the size of the coupling neighbourhood or the coupling topology. The task of selecting the coupling variables is performed here by the Orthogonal Forward Regression algorithm [4].

The symmetry of the coupling topology and of the coupling functions can be enforced explicitly during the selection stage. When polynomial models are used, F can be split into two parts

$$F(q^{n_y} y_i(t), q^{n_u} u_i(t), s^m q^{n_y} y_i(t), s^m q^{n_u} u_i(t)) = \quad (41)$$

$$F_l(q^{n_y} y_i(t), q^{n_u} u_i(t)) + F_c(q^{n_x} y_i(t), q^{n_u} u_i(t), s^m q^{n_y} y_i(t), s^m q^{n_u} u_i(t)) \quad (42)$$

where F_l involves only the input and outputs at i th lattice node and F_c is a function of neighbouring outputs but can also include cross-product terms of y_i . In this case, the candidate regressor set can be modified accordingly in order to ensure the symmetry of the coupling function F_c in the identified model. The idea is to replace the standard polynomial regressors that make up F_c with symmetric combinations of the respective polynomial terms.

If data is available from more sensors than minimum required to extract the CML equations (when data represent pixels in an image for example), the additional measurements will be used in model validation. The CML model identified using a set of data from a given spatial location can be validated on data recorded at different spatial locations by computing the model predicted output

$$\hat{y}_i(t) = F_l(q^{n_y} \hat{y}_i(t), q^{n_u} u_i(t)) + F_c(q^{n_y} \hat{y}_i(t), q^{n_u} u_i(t), s^m q^{n_y} \hat{y}_i(t), s^m q^{n_u} u_i(t)) \quad (43)$$

for the entire CML, $i \in \mathcal{I}$.

The additional data can also be merged and used in identification. Because of the spatial invariance of the input/output equations at each lattice node, structure selection can be performed by collecting all available data into an extended regression matrix.

4 Simulation Results

The identification procedure described in the previous section will be tested using simulated data from linear and nonlinear PDEs.

4.1 Example 1; A Linear Diffusion Equation

Consider the following diffusion equation

$$\frac{\partial^2 v(t, x)}{\partial t^2} - C \frac{\partial^2 v(t, x)}{\partial x^2} = u(t, x), \quad x \in [0, 1] \quad (44)$$

with initial conditions

$$\begin{aligned} v(0, x) &= 0 \\ \frac{dv(0, x)}{dt} &= 4 \exp(-x) + \exp(-0.5x) \end{aligned} \quad (45)$$

where

$$u(t, x) = -13 \exp(-x) \cos(1.5t) - 9.32 \exp(-0.5x) \cos(2.1t) \quad (46)$$

For $C = 1.0$ the exact solution $v(t, x)$ of the initial value problem (44), (45) is

$$\begin{aligned} v(t, x) &= 4 \exp(-x) \cos(1.5t) + 2 \exp(-0.5x) \cos(2.1t) - \\ &4 \exp(-x) \exp(-t) - 2 \exp(-x) \exp(-0.5t) \end{aligned} \quad (47)$$

The measurement function is taken as

$$y(t, x) = v(t, x) \quad (48)$$

The main advantage of using this PDE is that the identification method can be tested on the exact solution.

The reference solution was sampled at 21 equally spaced points over the spatial domain $\Omega = [0, 1]$, $x = (x_1, \dots, x_{21}) = (0, 0.05, \dots, 0.95, 1)$. From each location, 1000 input/output data points sampled at $\Delta t = \pi/100$ were generated. The data are plotted in Fig.(1) and Fig.(2) respectively.

The identification data consisted of 1000 data points of input/output output data $u_i(t)$ and $y_i(t)$ at node $i = 3$ corresponding to $x = x_3 = 0.1$. In addition, 1000 input and output data $u_{i-1}(t)$, $u_{i+1}(t)$, $y_{i-1}(t)$ and $y_{i+1}(t)$ from neighbouring locations $x = x_2 = .05$ and $x = x_4 = .15$ acted as inputs during the identification.

The following linear input/output equation was identified from the data

Terms	Estimates	$[ERR]_i$	Std. Dev.
$y_i(t-1)$	$0.11888E+1$	$0.99748E+0$	$0.27092E-9$
$y_i(t-2)$	$-0.97784E+0$	$0.25154E-2$	$0.26466E-9$
$u_i(t-1)$	$0.97170E-3$	$0.14195E-5$	$0.17908E-13$
$y^*(t-1)^a$	$0.40552E+0$	$0.75450E-7$	$0.13500E-10$
constant	$0.75114E-15$	$0.43172E-16$	$0.76589E-15$
$u_i(t-2)$	$0.14685E-4$	$0.33728E-17$	$0.17490E-12$
$y^*(t-2)^b$	$-0.11040E-1$	$0.41043E-15$	$0.13188E-9$

Table 4.1

$$^a y^*(t-1) = y_{i-1}(t-1) + y_{i+1}(t-1)$$

$$^b y^*(t-2) = y_{i-1}(t-2) + y_{i+1}(t-2)$$

The model set was defined such that the estimated lattice equations have a symmetric coupling topology. In addition, model terms of the form $y^*(t-k) = y_{i-1}(t-k) + y_{i+1}(t-k)$ were included in the model set, to replace the original linear terms, in order to ensure that the estimated coefficients of $y_{i-1}(t-1)$ and $y_{i+1}(t-1)$ as well as of $y_{i-1}(t-2)$ and $y_{i+1}(t-2)$ are identical.

Equations (4.1) were used to implement a one-dimensional CML model with 21 lattice nodes. Since in principle the CML model corresponding to (44) is infinite dimensional, the reference solutions computed at $x = -0.05$ and $x = 1.05$, $y_0(t)$ and $y_{22}(t)$ respectively, were used as boundary conditions in the simulation.

The model predicted output defined in (43) is plotted in Fig.(3) for comparison. The model predicted errors (not the fitting error) in Fig. (4) show excellent agreement between the exact solution and the CML model output.

4.2 Example 2: A Nonlinear Reaction-Diffusion Equation

In this example, a nonlinear reaction-diffusion equation, namely the FitzHugh-Nagumo equation

$$\frac{\partial u_1}{\partial t} = d_1 \frac{\partial^2 u_1}{\partial x^2} + g(u_1) - u_2 \quad (49)$$

$$\frac{\partial u_2}{\partial t} = d_2 \frac{\partial^2 u_2}{\partial x^2} + \delta u_1 - \gamma u_2 \quad (50)$$

with $x \in \Omega = [0, 1]$ and Dirichlet boundary conditions (i.e. $u_1(t, 0) = u_1(t, 1) = u_2(t, 0) = u_2(t, 1) = 0$), was used to test the identification approach. This equation was originally introduced to describe the conduction of nerve impulses along the axon [14], [29].

In equation (49) $g(u_1) = -u_1(u_1 - \alpha)(u_1 - 1)$ with u_1 representing the electrical potential in the axon. The other variable u_2 has a more complicated interpretation.

The PDE was simulated with high accuracy for the following parameter values, $d_1 = d_2 = 6.188e - 4$, $\delta = 40$ and $\gamma = -0.2$. and with initial conditions

$$\begin{aligned} u_1(0, x) &= \sin(\pi x/2) \\ u_2(0, x) &= \sin(\pi x/2) \end{aligned} \quad (51)$$

The measurement function was taken as

$$y(t, x) = u(t, x) \quad (52)$$

where $y = (y_1(t, x), y_2(t, x))$ and $u(t, x) = (u_1(t, x), u_2(t, x))$. The identification was carried out using 1000 data samples of y_{i-1}, y_i, y_{i+1} recorded at the spatial locations $(x_{i-1}, x_i, x_{i+1}) = \{.04, .06, .08\}$, $i = 2, 3, 4$, with $y_i(t) = (y_{1,i}(t), y_{2,i}(t)) = (u_1(t, x_i), u_2(t, x_i))$. As in the previous example the outputs y_{i-1} and y_{i+1} were considered as inputs during identification of the lattice equation corresponding to $i = 3$.

The model identified from data, based on a cubic polynomial model set of 2×35 polynomial terms, is listed in table (4.2)

Output	Terms	Estimates	$[ERR]_i$	Std. Dev.
$y_{1,i}(t)$	$y_{1,i}^*(t-1)^a$	$0.18460E - 1$	$0.99680E + 0$	$0.75148E - 3$
	$y_{2,i}(t-1)$	$-0.10072E - 1$	$0.29226E - 2$	$0.17522E - 5$
	$y_{1,i}^{*2}(t-1)$	$0.31508E - 2$	$0.22672E - 3$	$0.18541E - 5$
	$y_{1,i}^{*3}(t-1)$	$-0.12084E - 2$	$0.34372E - 4$	$0.23414E - 5$
	$y_{1,i}(t-1)$	$0.95797E + 0$	$0.12619E - 4$	$0.14885E - 2$
	$y_{1,i}(t-1)y_{2,i}^2(t-1)$	$-0.75019E - 5$	$0.30001E - 6$	$0.51894E - 6$
	$y_{2,i}^2(t-1)$	$0.18601E - 5$	$0.12262E - 7$	$0.12683E - 6$
	$y_{1,i}^2(t-1)y_{2,i}(t-1)$	$0.34816E - 2$	$0.16093E - 7$	$0.15411E - 3$
	$y_{1,i}(t-1)y_{2,i}(t-1)$	$-0.84444E - 4$	$0.47418E - 7$	$0.25826E - 5$
	$y_{2,i}(t-1)y_{1,i}^{*2}(t-1)$	$-0.85966E - 3$	$0.11930E - 7$	$0.39460E - 4$
$y_{2,i}(t)$	$y_{2,i}^*(t-1)^b$	$0.23714E - 1$	$0.99722E + 0$	$0.16171E - 2$
	$y_{1,i}(t-1)$	$0.39946E + 0$	$0.27625E - 2$	$0.12987E - 3$
	$y_{2,i}(t-1)$	$0.97093E + 0$	$0.11998E - 4$	$0.321262E - 2$
	const.	$0.23277E - 2$	$0.12459E - 6$	$0.75939E - 4$

Table 4.2

$$^a y_{1,i}^*(t-1) = y_{1,i-1}(t-1) + y_{1,i+1}(t-1)$$

$$^b y_{2,i}^*(t-1) = y_{2,i-1}(t-1) + y_{2,i+1}(t-1)$$

The symmetry of the coupling topology and of the coupling functions was ensured by modifying the original regressor set to include only symmetrical polynomial terms relative to y_{i-1} and y_{i+1} .

The identified equations (4.2) were used to implement a CML model with 49 nodes which was simulated using the Dirichlet boundary conditions. The reference solution and the model predicted output plotted in Figs.(5a,b) and Figs.(6a,b) are in excellent agreement. The error surfaces are shown in Figs.(7).

5 Conclusions

New algorithms have been introduced, which for the first time allow the identification of Coupled Map Lattice models of spatially extended systems directly from data. The proposed identification method can be successfully applied to identify linear or nonlinear evolution equations.

The new algorithm was formulated by adapting the NARMAX method, originally developed for the identification of lumped parameter nonlinear dynamical systems, to accommodate spatially distributed data.

The new approach exploits the spatial invariance property of the CML equations to identify finite or infinite dimensional CML models from data recorded at only a few spatial locations. Additional constraints such as coupling symmetry are also handled by the new structure selection algorithm.

The identified input/output equations at one node can then be used to reconstruct the global dynamics subject to some mild assumptions regarding the measurement function.

The applicability of the new approach has been illustrated using noise-free simulated data for two partial differential equations. The identification of the CML in a stochastic context will be addressed in a separate study.

6 Acknowledgment

The authors gratefully acknowledge that this research was supported by the UK Engineering and Physical Sciences Research Council.

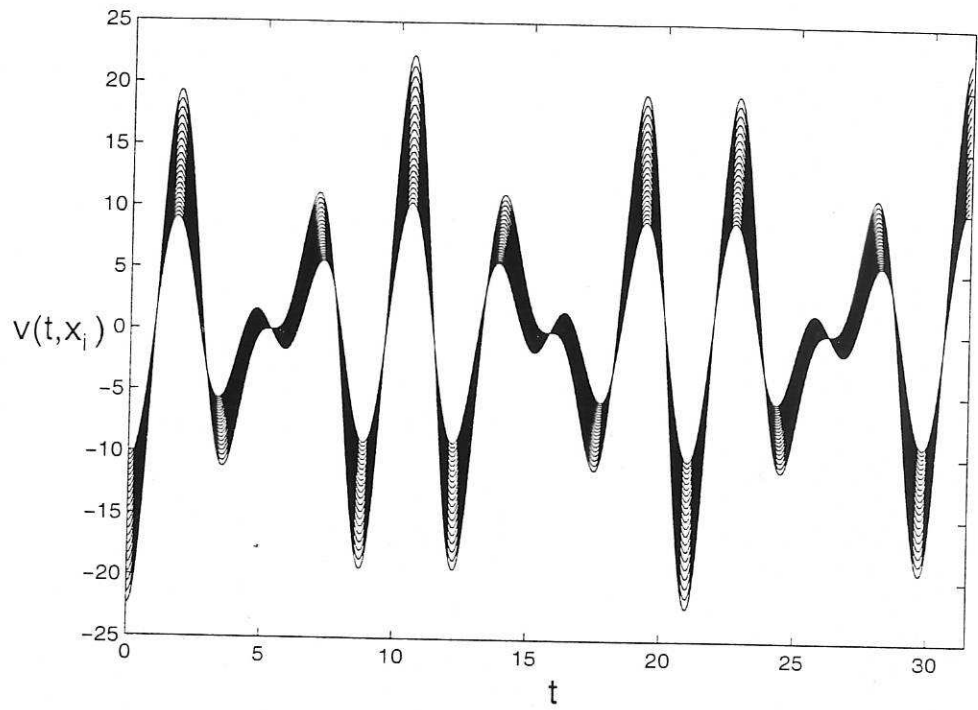


Figure 1: Example 1, Simulated input data $v(t, x)$: $dt = \pi/100$, $x = [0.05, 0.01, \dots, 1]$

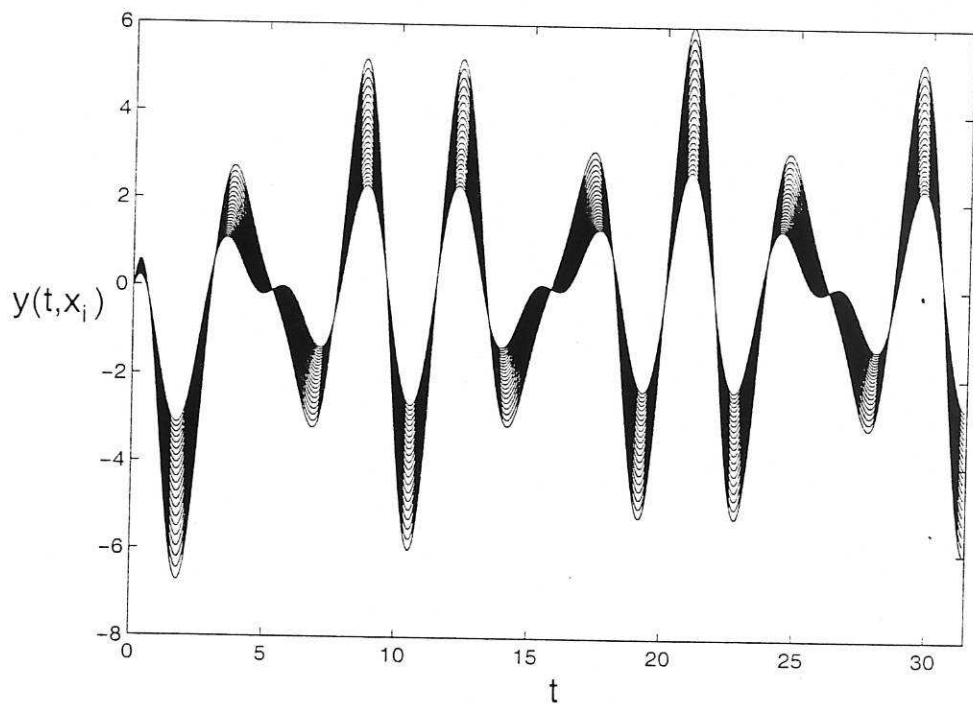


Figure 2: Example 1, Simulated output data $y(t, x)$: $dt = \pi/100$, $x = [0.05, 0.1, \dots, 1]$

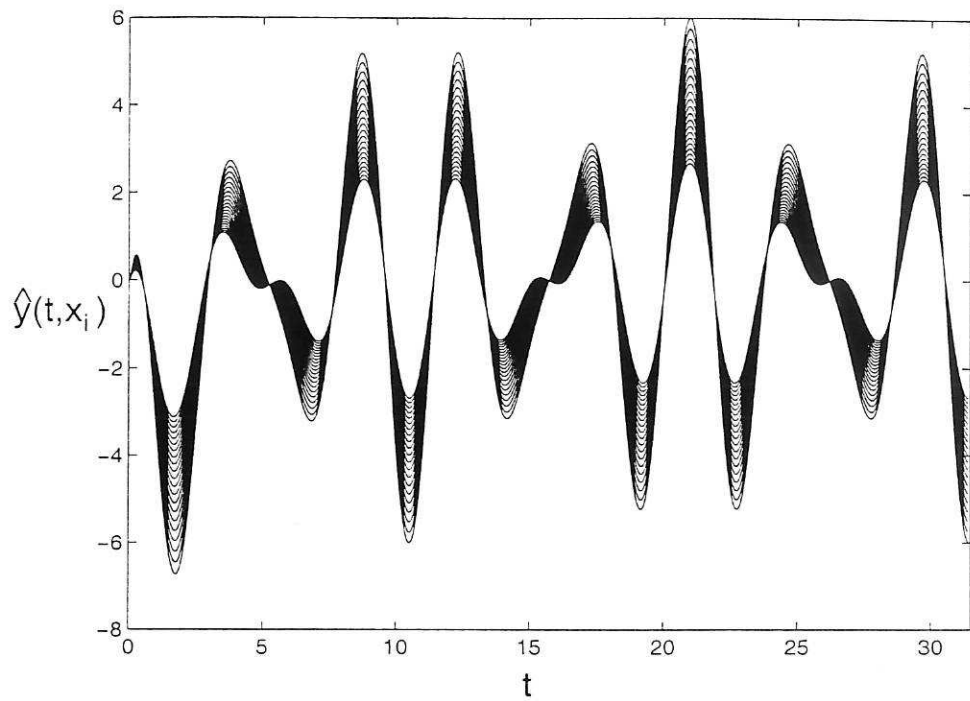


Figure 3: Example 1, Model predicted PDE solution $\hat{y}(t, x_i)$ for $i = 1, \dots, 21$

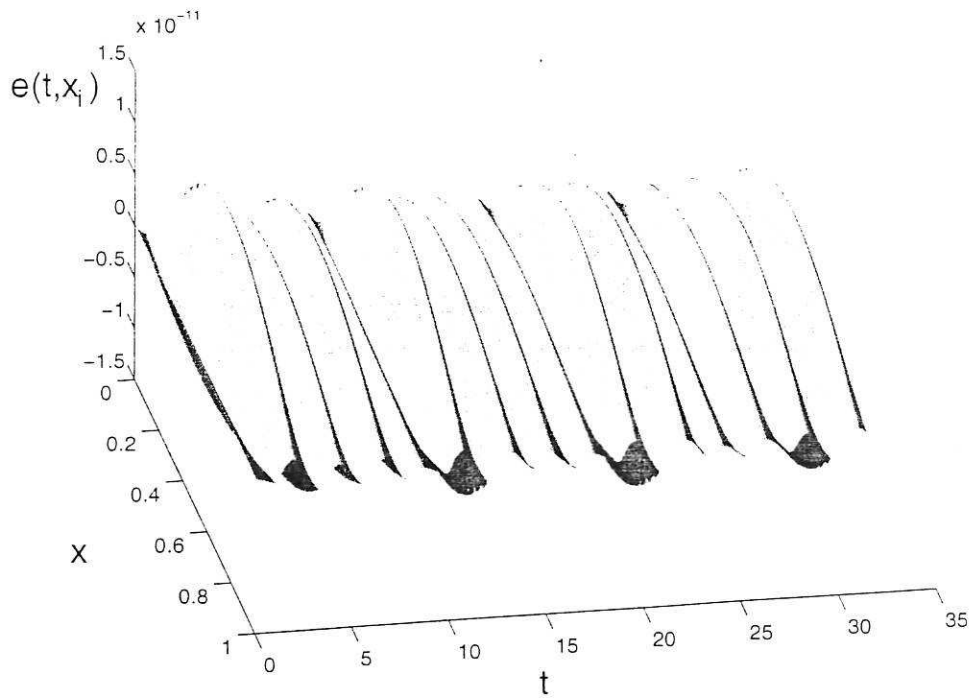


Figure 4: Example 1, Model predicted error $e(t, x_i) = y(t, x_i) - \hat{y}(t, x_i)$

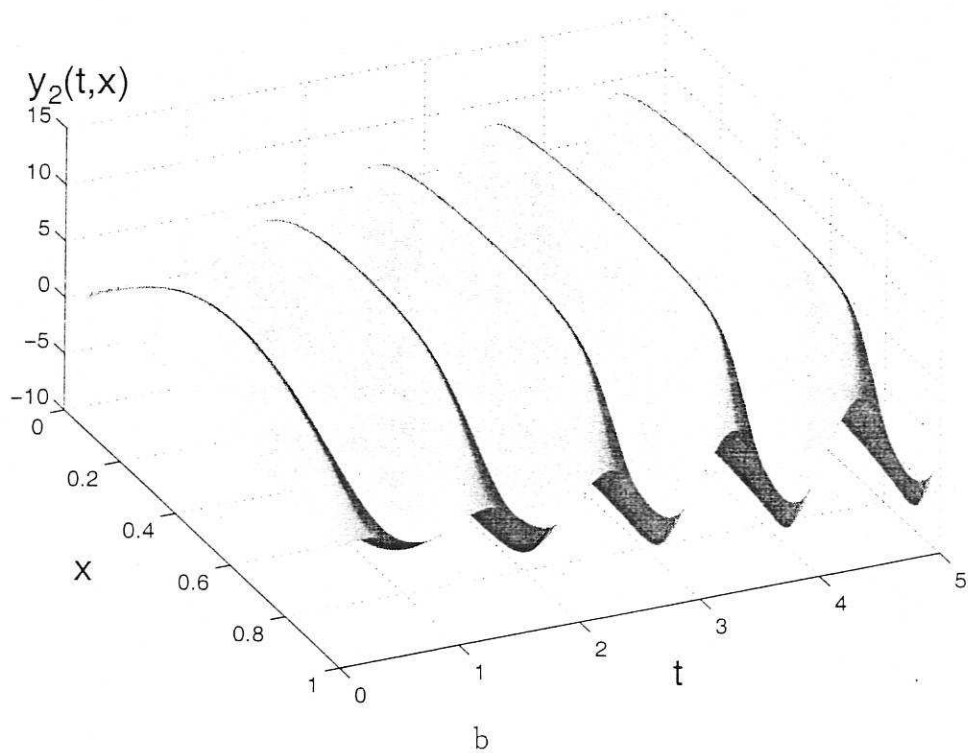
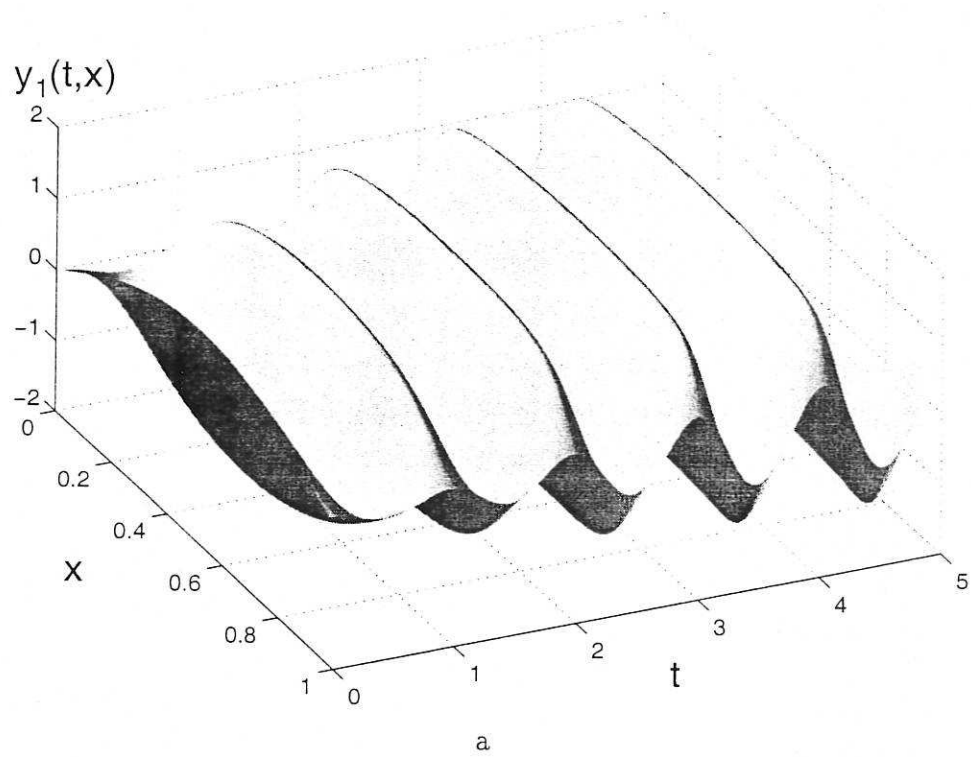


Figure 5: Example 2, Simulated data for the FitzHugh-Nagumo Equations: a) $y_1(t, x)$ b) $y_2(t, x)$

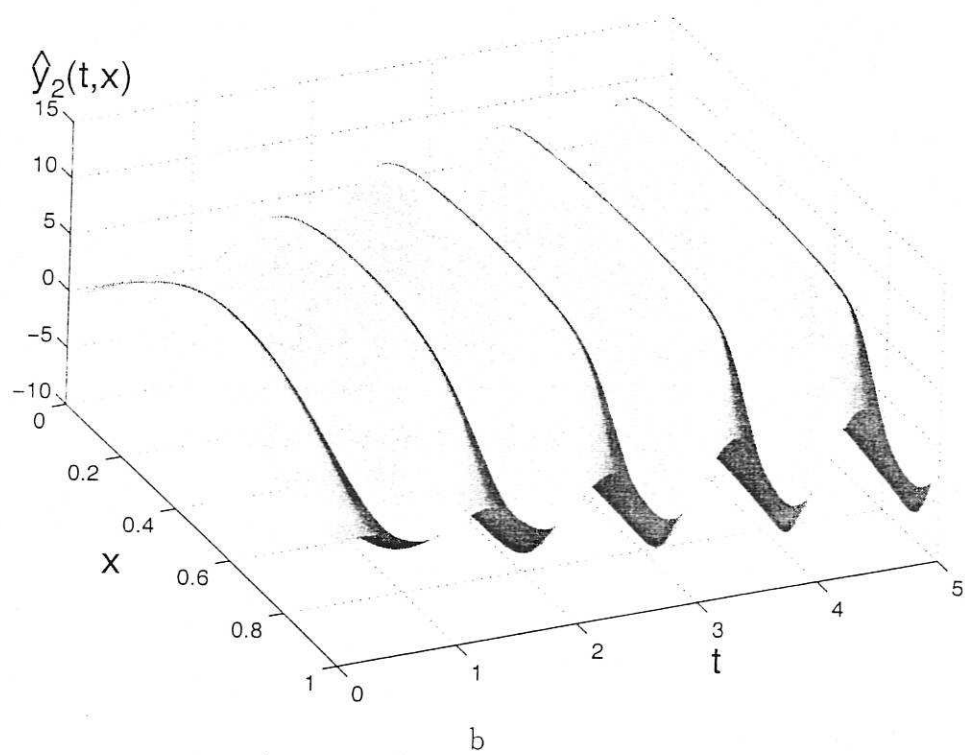
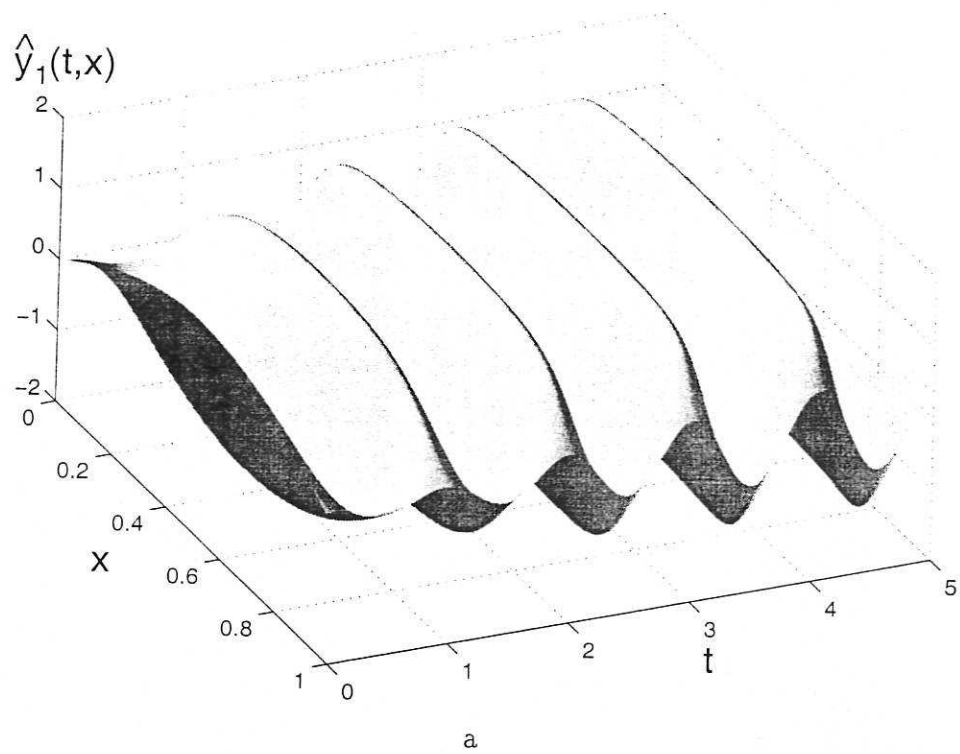


Figure 6: Example 2, Model predicted PDE solutions: a) $\hat{y}^1(t, x_k)$, b) $\hat{y}^2(t, x_k)$

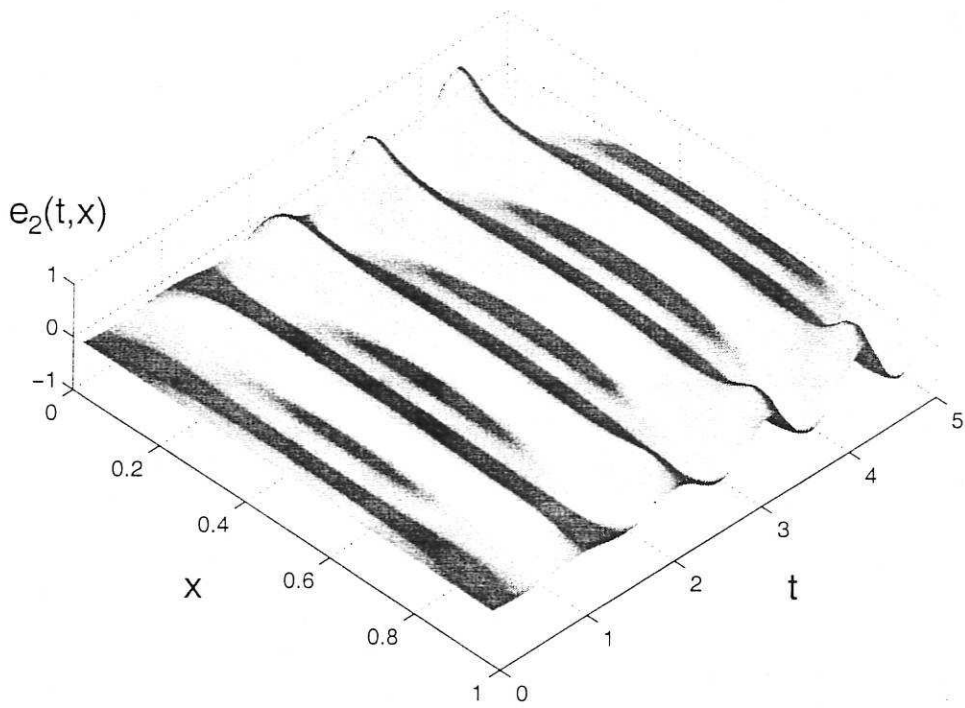
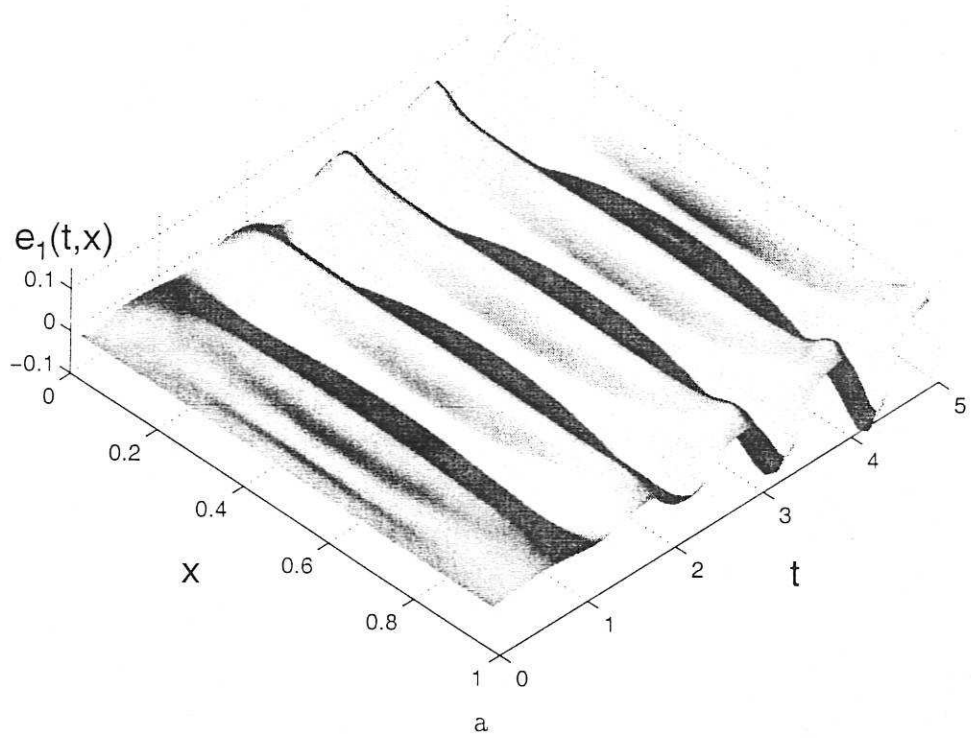


Figure 7: Example 2, Model prediction errors: a) $e_1(t,x) = y_1(t,x) - \hat{y}_1(t,x)$ b) $e_2(t,x) = y_2(t,x) - \hat{y}_2(t,x)$

- [15] E. P. Goodson and M. P. Polis. Identification of parameters in distributed systems. In W. H. Ray and D. G. Lainiotis, editors, *Distributed Parameter Systems. Identification, Estimation and Control*, pages 47–133. Marcel Dekker, New York, 1978.
- [16] C. M. Gray, P. König, and A. K. Engel. Oscillatory responses in cat visual cortex exhibit inter-columnar synchronisation which reflects global stimulus properties. *Nature*, 338:334–337, 1989.
- [17] G. He, L. Cao, and J Li. Convective coupled map for simulating spatiotemporal chaos in flows. *Acta Mechanica Sinica*, 11:1–7, 1995.
- [18] A. L. Hodgkin and A. F. Huxley. A quantitative description of membrane current and its application to conduction and excitation in nerves. *J. Physiology*, 117:500–544, 1953.
- [19] A. Isidori, editor. *Nonlinear Control Systems*. Springer Verlag, Berlin, 1995.
- [20] J. Jalife and G. K. Moe. Excitation, conduction and reflection of impulses in isolated bovine and canine cardiac purkinje fibers. *Circulation Res.*, 49:233–247, 1981.
- [21] K Kaneko. Spatiotemporal intermittency in coupled map lattices. *Progress of Theoretical Physics*, 74(5):1033–1044, 1985.
- [22] K Kaneko. Turbulence in coupled map lattices. *Physica D*, 18:475–476, 1986.
- [23] K Kaneko. Pattern dynamics in spatiotemporal chaos. pattern selection, diffusion of defect and pattern competition intermittency. *Physica D*, 34:1–41, 1989.
- [24] K. Kaneko, editor. *Coupled Map Lattices: Theory and Experiment*. World Scientific, Singapore, 1993.
- [25] J. P. Keener. Propagation and its failure in coupled systems of discrete excitable cells. *J. Appl. Mathematics*, 47:556–572, 1987.
- [26] J. P. Keener. A mathematical model for the vulnerable phase in myocardium. *Mathematical Biosciences*, 90:31–38, 1988.
- [27] I. J. Leontaritis and S. A. Billings. Input-output parametric models for non-linear systems - Part II: Stochastic non-linear systems. *Int. J. Control*, 41:329–344, 1985.
- [28] I. J. Leontaritis and S. A. Billings. Input-output parametric models for non-linear systems- Part I: Deterministic non-linear systems. *Int. J. Control*, 41:303–328, 1985.
- [29] J. Nagumo, S. Arimoto, and S. Yoshizawa. Bistabile transmission lines. *IEEE Trans. Circuit Theory*, 12:400–412, 1965.
- [30] K. Otsuka. Complex dynamics in coupled nonlinear element systems. *Int. J. of Modern Phys. B*, 8(5):1179–1214, 1991.



- [31] N. Platt and S. Hammel. Pattern formation in driven coupled map lattices. *Physica A*, 239(1-3):296-303, 1997.
- [32] R. V. Sole, J. Valls, and Bascompte J. Spiral waves, chaos and multiple attractors in lattice models of interacting populations. *Physics Letters A*, 166(2):123-128, 1992.
- [33] R. Temam. *Infinite-Dimensional Dynamical Systems in Mechanics and Physics*, volume 68 of *Applied Mathematical Sciences*. Springer Verlag, 1988.
- [34] A. J. van der Shaft. On realization of nonlinear systems described by higher-order differential equations. *Math. Systems Theory*, 19:239-275, 1987.
- [35] T. Yanagita. Phenomenology of boiling: A coupled map lattice model. *Chaos*, 2(3):343-350, 1992.
- [36] Y Zhou and J. Bell. Study of propagation along nonuniform excitation fibres. *Mathematical Biosciences*, 119:169-203, 1994.